Available online at www.sciencedirect.com
ScienceDirect
Chinese Journal of Natural Medicines 2019, **17**(10): 0768–0777
Chinese Journal of Natural Medicines

Inhibitory effects of polyphyllins I and VII on human cisplatin-resistant NSCLC *via* p53 upregulation and CIP2A/AKT/mTOR signaling axis inhibition

FENG Fei-Fei[1Δ], CHENG Peng[2Δ], SUN Chao[3], WANG Hui[1], WANG Wei[1*]

[1] *Department of Respiratory Medicine, The Second Hospital of Shandong University, Jinan 250033, China;*
[2] *Department of Neural Medicine, The Second Hospital of Shandong University, Jinan 250033, China;*
[3] *Department of Central Laboratory, The Second Hospital of Shandong University, Jinan 250033, China*

Available online 20 Oct., 2019

[ABSTRACT] Cancerous inhibitor of protein phosphatase 2A (CIP2A) is a human oncoprotein that is overexpressed in multiple kinds of cancers including non-small cell lung cancer (NSCLC). CIP2A plays an 'oncogenic nexus' to participate in the tumorigenesis and chemoresistance in several cancer types. AKT and mTORC1 overactivation are detected in NSCLC and many other cancers. Previous studies found that the CIP2A/AKT/mTOR pathway controls cell growth, apoptosis, autophagy process. Polyphyllin I (PPI) and polyphyllin VII (PPVII) are natural components extracted from *Paris polyphylla* that display anti-cancer properties. In the present study, we investigated whether PPI and PPVII can be used in the cisplatin (DDP)-resistant human NSCLC cell line A549/DDP. Results demonstrated that PPI and PPVII treatment significantly suppressed A549/DDP cell proliferation, migration, invasion and EMT, induced apoptosis and autophagy. Further examination of the mechanism revealed that the PPI and PPVII significantly upregulated the p53, induced caspase-dependent apoptosis and suppressed the CIP2A/AKT/mTOR pathway. The activation of autophagy was mediated through PPI and PPVII induced inhibition of mTOR. We propose that PPI and PPVII might be developed as candidate drugs for DDP-resistant NSCLC.

[KEY WORDS] Polyphyllin I; Polyphyllin VII; Cisplatin-resistance; Non-small cell lung cancer; p53; Cancerous inhibitor of protein phosphatase 2A

[CLC Number] R965 **[Document code]** A **[Article ID]** 2095-6975(2019)10-0768-11

Introduction

Lung cancer is still the leading cause of cancer related deaths worldwide. Non-small cell lung cancer (NSCLC) is the most common type, accounts for about 85% of all cases of lung cancers. Nearly 70% of patients with NSCLC are in advanced or metastatic phase when diagnosed and the 5-year survival rate is less than 5% [1]. Surgery, chemotherapy, radiation therapy, and targeted therapies are current treatments for NSCLC patients, of which platinum-based chemotherapy plays a critical role in advanced or metastatic lung cancer treatment [2]. Cisplatin (DDP) is one of the first-line chemotherapeutic agent for lung cancer. However, due to congenital or acquired resistance, the response rate of cisplatin treatment against advanced NSCLC remains unsatisfactory. Also, chemotherapy is often limited by dose-related toxicity, which restricts its clinical application, therefore, developing new therapeutic agents which are more effective and less toxic is urgently needed. Natural compounds that diminish the side effects of chemotherapy agents demonstrate a novel source of anticancer alternatives.

Cancerous inhibitor of protein phosphatase 2A (CIP2A), one of the most important endogenous inhibitor of protein phosphatase 2A (PP2A), is a novel human oncoprotein that is overexpressed in multiple cancer types including NSCLC [3-7]. Previous independent studies have demonstrated that CIP2A is capable to promote the proliferation and aggressiveness of cancer cells and its over-expression was associated with tumor growth, drug resistance, apoptosis resistance, metastasis,

[Received on] 05-Aug.-2019
[Research funding] This work was supported by the National Natural Science Foundation of China (No. 81473485) and the Natural Science Foundation of Shandong Province (No. 2014ZRE27321).
[*Corresponding author] Tel: 86-531-85875572, E-mail: sducp@qq.com
[Δ] These authors contributed equally to this work.
These authors have no conflict of interest to declare.
Published by Elsevier B.V. All rights reserved

and might be a predictive factor of poor prognosis in many human solid malignancies [6-7]. Mechanically, CIP2A plays an 'oncogenic nexus' to participate in the tumorigenesis and chemoresistance in several cancer types [6]. CIP2A stabilizes c-Myc and activates AKT by inhibiting PP2A-mediated dephosphorylation of c-Myc and AKT [7]. This function consequently makes CIP2A able to exert its influence on signaling pathways such as PI3K-AKT-mTOR pathway and RAS-MEK-ERK pathway. It has been reported that CIP2A cooperates with the oncogene H-Ras *via* the MEK/ERK pathway to facilitate the EMT process in cervical cancer [8]. CIP2A can also associate with mTOR directly and act as an allosteric inhibitor of mTORC1-associated PP2A, while mTORC1 is the major negative regulator of autophagy and its activation results in phosphorylation of important effectors involved in cancer progression and apoptosis resistance [9]. Moreover, CIP2A could mediate the anticancer effects of several compounds including bortezomib and erlotinib by inhibiting AKT-related PP2A activity and activating p-AKT [10-11]. Notably it also has been proved that CIP2A mediated AKT phosphorylation plays a role in DDP resistance [12]. Therefore, targeting CIP2A might be an attractive therapeutic strategy for DDP-resistant NSCLC treatment.

Rhizoma of *Paris polyphylla* (RPS) is a traditional Chinese medicinal herb which exhibits a wide range of pharmacological properties, including immunity-enhancing, anti-inflammatory, and anticancer effects [13]. At present, various steroidal saponins have been identified to be the active components isolated from RPS. Among these compounds, Polyphyllin I (PPI) displayed a strong inhibitory effect on varies cancers, including ovarian cancer [14], hepatocarcinoma [15], ovarian cancer [16], osteosarcoma [17], non-small cell lung cancer [18], gastric cancer [19] and so forth. By inducing apoptosis and autophagy, triggering cell cycle arrest, demonstrating anti-angiogenic effects, PPI ultimately suppress the proliferation and metastasis of tumor cells. Successively, Polyphyllin VII (PPVII) also exerts anticancer effects on oral cancer [20], hepatocellular carcinoma [21], lung cancer [22] by regulating the signal pathways associated with proliferation, apoptosis and autophagy. However, so far, fewer studies of PPI and PPVII have been undertaken on acquired DDP-resistant NSCLC. In this study we determined the anti-cancer effects of PPI and PPVII on A549/DDP cells *in vitro* and further explored the possible molecular mechanisms.

Materials and Methods

Experimental reagents

PPI (molecular formula $C_{44}H_{70}O_{16}$, molecular weight 855.02, lot no. B-21668, HPLC ≥ 98%) and PPVII (molecular formula $C_{51}H_{82}O_{21}$, molecular weight 1031.2, lot no. B-50583, HPLC ≥ 95%) were purchased from Shanghai Source Leaf Biotechnology Co., Ltd. (Shanghai, China) and dissolved in dimethylsulfoxide (DMSO) to a concentration of 50 mg·mL^{-1}. After filter sterilization, the solution was preserved at –20 °C. The solution was added with culture medium to a final concentration of less than 1% DMSO. Cisplatin was purchased from Sigma-Aldrich (St. Louis, MO, USA). Cell Counting Kit-8 (CCK-8) assay kits were purchased from Dojindo China Co., Ltd.. The Annexin V Apoptosis Detection Kit was purchased from BD Biosciences (San Diego, CA, USA). The antibodies for western blotting, i.e. anti-CIP2A, anti-AKT, anti-phosphorylated AKT (p-AKT), anti-mTOR, anti-phosphorylated mTOR (p-mTOR), anti-PARP, anti-cleaved PARP, anti-p53, anti-Bcl-2, anti-Bax, anti-caspase-3, anti-cleaved-caspase-3, anti-caspase-9, anti-cleaved-caspase-9 were purchased from Cell Signaling Technology (Danvers, MA, USA). Horseradish peroxidase–conjugated anti-mouse and anti-rabbit IgG antibody GAPDH were purchased from Zsbio Commerce Store (Beijing, China), Other reagents were purchased from local commercial suppliers.

Cell culture

A549 cells and A549/DDP cells (human non-small cell lung cancer cells) were obtained from the Zhongshan Golden Bridge Bio-technology Co., Ltd. (Beijing, China). A549 cells and A549/DDP cells were cultured in the RPMI-1640 medium (Gibco, Thermo Fisher Scientific Inc., MA, USA) supplemented with 10% of fetal bovine serum (BD Pharmingen, San Diego, CA, USA), 2% penicillin/streptomycin (10 000 U·mL^{-1} penicillin, 10 000 μg·mL^{-1} streptomycin), in an atmosphere containing 5% of CO_2 at 37 °C. cells used in all experiments were during the logarithmic growth phase. A549/DDP cells were grown in RPMI 1640 with 1000 ng·mL^{-1} cisplatin.

Cell proliferation and viability assays

The Cell Counting Kit-8 (CCK-8) assay was performed to assess the effect of PPI and PPVII on cell proliferation. Cells during logarithmic growth were adjusted to a cell density of 5.0 × 10^4/mL, then 100 μL was seeded in 96-well plates at a density of 5.0 × 10^3 cells/well, allowed cells to adhere for 24 h, followed by treatment with indicated drugs, after maintained in culture for 24 or 48 h, 100 μL sterile CCK-8 solution was added in the culture medium of each well, incubation at 37 °C for 1–4 h, then spectrometric absorbance at 450 nm was detected on a microplate reader.

The effect of each drug on cell viability was calculated according to the following formula: cell survival rate (cell viability) % = [*OD* of dosing group A /*OD* of control group A] × 100%, then cell viability curves were drawn with drug concentrations on the *X*-axis and average cell viability on the *Y*-axis. SPSS software (version 19.0) was employed to calculate the 50% inhibitory concentration (IC_{50}). All the experiments were repeated three times.

Annexin V-fluorescein isothiocyanate (FITC)/propidium iodide (PI) apoptosis analysis

A549/DDP cells were seeded in 6-well plates (5 × 10^4 cells/well), allowed cells to adhere for 24 h and then treated with indicated drugs for 24 h, then the cells were harvested and digested with trypsin without EDTA, after washed two times with cold PBS and resuspended in 100 μL of binding

buffer, 5 μL of annexin V–FITC and 5 μL of PI were added and the mixture was incubated in the dark for 15 min, then 400 μL of binding buffer was added to each tube and the cells were gently blended. Finally, fluorescence of the samples was analyzed using a flow cytometer (Accuri C6, BD Biosciences, San Diego, CA, USA) to detect apoptosis at 488/530 nm. Early apoptotic cells were Annexin V-FITC (+)/PI (–), while late apoptotic or necrotic cells were Annexin V-FITC (+)/PI (+).

Western blot analysis

After treatment with indicated drugs for 24 h, the cells were lysed with RIPA (Beyotime, Shanghai, China) lysis buffer (containing 2% Protease inhibitor, 2% phosphatase inhibitors and 2% EDTA) on ice for 30 min, then the cells were harvested and centrifuged at 12 000 ×*g* for 20 min. the supernatant were collected. The total protein concentration of each sample was detected by the BCA Protein Assay Kit (Beyotime, Shanghai, China). Samples containing equal quantity of protein were separated by electrophoresis with 10% SDS-PAGE, and then electro-transferred to polyvinylidene fluoride (PVDF) membranes (Millipore, Billerica, MA, USA) using a constant current of 180 mA for at least 120 min at 0 °C, after that, the PVDF membranes were blocked with 5% nonfat milk made with TBST (1 × Tris-buffered saline, 0.1% Tween 20), and then incubated with specific primary antibodies over night at 4 °C, followed by incubated with the horseradish peroxidase (HRP)-conjugated secondary antibody for 90 min at room temperature. After washing with TBST for 3 times, the bound antibody complexes were detected with the enhanced chemiluminescence reagent (ECL, Amersham Pharmacia Biotech, Piscataway, NJ, USA), then analyzed by Quantity One software, version 4.6 (Bio-Rad Laboratories). Expression of GAPDH served as a loading control.

Colony formation assay

A549/DDP cells during logarithmic growth was seeded in 6 cm diameter cell culture plates at a density of 5.0×10^2 cells/well in triplicate, incubated with indicated drugs except for the control group. After 2 weeks, the cells were fixed with 4% paraformaldehyde at 4 °C for 60 min, then stained with 0.2% gentian violet and the colonies were counted under a light microscope at ×70 objective (1 × 70; Olympus Corp, Tokyo, Japan).

Wound healing assay

A549/DDP cells were seeded in 6-well plates at a density of 4.0×10^5 cells/well and incubated at 37 °C until 90% to 100% confluence. Next the confluent cells were scratched with a 200 μL pipette tip, followed by washing with PBS, and then treated with indicated drugs with a complete medium. After 24 h of incubation, randomly chosen fields were photographed under a light microscope at ×4 objective. The number of cells migrated into the scratched area was calculated.

Invasion assay

A 24-well plate with polyvinyl-pyrrolidone-free polycarbonate filters (8 μm pore size) (Corning) was used for invasion assay. The filters were coated with Matrigel (BD Biosciences). The lower chamber was added with 600 μL medium containing 20% FBS as chemoattractant, the upper chamber with coated filter was laid over the lower chamber. 100 μL A549/DDP cell suspension (5×10^4 cells) containing different concentrations of PPI or PPVII was seeded onto the upper chamber well respectively. After incubation at 37 °C for 24 h, the filter was fixed with 4% paraformaldehyde for 30 min and stained with 0.2% gentian violet for 20 min. Then the upper unmigrated cells were gently wiped off by a cotton swab, followed by washing with PBS for three times. After being dried, the lower migrated cells on the membrane were enumerated under a light microscope at ×10 objective.

Statistical analysis

All experiments were repeated at least three times and the data were processed by SPSS 19.0 software (IBM SPSS, Armonk, NY, USA). The relative expression was represented as the mean ± SD. Differences between data groups were evaluated for significance using Student's *t*-test of unpaired data or one-way analysis of variance and Bonferroni post hoc test. *P*-values < 0.05 indicate statistical significance.

Result

Chemical structure of PPI and PPVII and characterization of A549 and A549/DDP cells

Firstly, A549 and A549/DDP cells were exposed to different concentrations of DDP (1–32 $\mu g \cdot mL^{-1}$) for 24 h. The 50% inhibitory concentration (IC_{50}) of DDP against A549 cells is 5.49 $\mu g \cdot mL^{-1}$, while IC_{50} of DDP against A549/DDP cells is 33.36 $\mu g \cdot mL^{-1}$. As shown in Fig. 1A, the cisplatin cytotoxicity in A549 cells was higher than in A549/DDP cells. Then, the CIP2A, p-AKT, AKT, p-mTOR was compared between A549 and A549/DDP cells, which confirmed CIP2A, p-AKT, AKT, p-mTOR were overexpressed in A549/DDP cells (Fig. 1B).

Inhibitory effects of PPI and PPVII on A549 and A549/DDP cells

A549 and A549/DDP cells were seeded in 96-well plates for 24 h and then treated with different concentrations of PPI (Figs. 2A–2C) and PPVII (Figs. 2D–2F). After 24 h, the cell viability was determined by CCK-8 assay. Absorbance at 450 nm was detected on a microplate reader. We found that PPI and PPVII caused moderate cytotoxicity in A549 and A549/DDP cells, the IC_{50} of PPI on A549 and A549/DDP cells were 1.54 ± 0.26 and 1.08 ± 0.20 $\mu g \cdot mL^{-1}$, while the IC_{50} values of PPVII on A549 and A549/DDP cells were 2.26 ± 0.30 and 1.84 ± 0.23 $\mu g \cdot mL^{-1}$ respectively (Table 1). We found that PPI and PPVII reduced viable A549/DDP cells in a dose and time dependent manner (Figs. 2A–2F).

We also investigated the effect of PPI and PPVII on cell colony formation and found that PPI (Fig. 2G) and PPVII (Fig. 2H) significantly inhibited the clonogenic ability of A549/DDP. These results suggested that PPI and PPVII inhibited both the anchorage-dependent growth (cell proliferation) and anchorage-independent growth (colony formation) of A549/DDP cells.

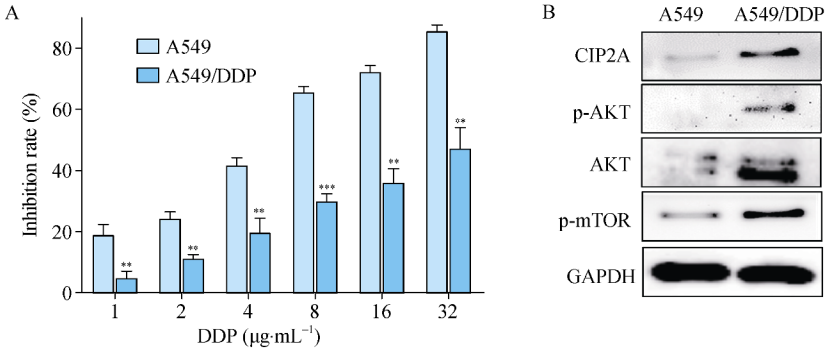

Fig. 1 Characterization of A549 and A549/DDP cells. (A) Cell viability was determined by CCK-8 assay in A549 and A549/DDP cells after incubation with different doses of cisplatin for 24 h. $^{**}P < 0.01$, $^{***}P < 0.001$ *vs* A549 group; (B) Western blotting analysis showing protein expression in A549 and A549/DDP cells using the antibodies indicated

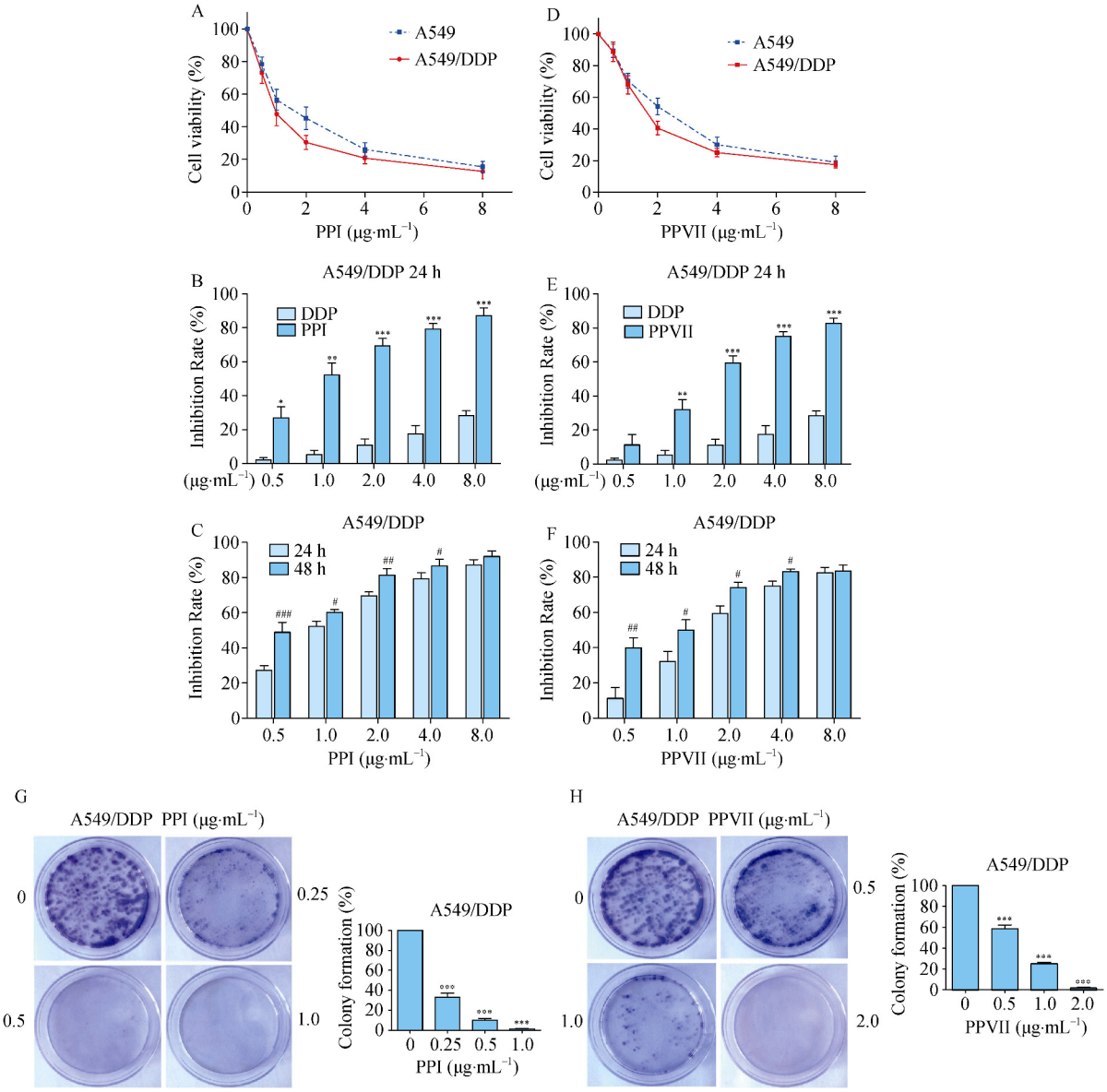

Fig. 2 Effect of PPI and PPVII on A549 and A549/DDP cells. (A–F) The inhibitory effects of PPI (A–C) and PPVII (D–F) on A549 and A549/DDP cells analyzed by CCK-8 assay. $^{*}P < 0.05$, $^{**}P < 0.01$, $^{***}P < 0.001$ *vs* cisplatin group; $^{\#}P < 0.05$, $^{\#\#}P < 0.01$, $^{\#\#\#}P < 0.001$ *vs* 24 h group. (G, H) The colony formation assays of A549/DDP cells treated with PPI (G) and PPVII (H) at the indicated concentration. $^{*}P < 0.05$, $^{**}P < 0.01$, $^{***}P < 0.001$ *vs* control group

PPI and PPVII inhibit migration, invasion and reverse EMT in A549/DDP cells

EMT is recognized as an important process that occurs during NSCLC cell invasion and migration, as well as drug resistance [23]. We determined whether PPI and PPVII could influence EMT process in A549/DDP cells. we first examined invasive behavior. As shown in Fig. 3, PPI (Fig. 3A) and PPVII (Fig. 3B) markedly suppressed the migration of A549/DDP cells. Then an invasion assay was carried out, PPI (Fig. 3C) and PPVII (Fig. 3D) also significantly suppressed the invasion of A549/DDP cells. Subsequently, we assessed the expression of EMT markers by western blot analysis after PPI and PPVII treatment. The results revealed that treatment of A549/DDP cells with PPI (Fig.3E) and PPVII (Fig.3F) reverse EMT, as evidenced by upregulation of epithelial marker E-cadherin and down-regulation of the mesenchymal markers vimentin, *α*-SMA. These data demonstrate that PPI and PPVII reverse EMT, in part, to suppress the migration and invasion of A549/DDP cells.

PPI and PPVII induces apoptosis in A549/DDP cells

To investigate whether PPI and PPVII induced apoptosis in A549/DDP cells, we measured apoptotic A549/DDP cells using the FITC Annexin V Apoptosis Detection Kit according to the manufacturer's instructions. Early apoptotic cells were Annexin V-FITC-positive and PI-negative, while late apoptotic or necrotic cells were Annexin V-FITC-positive and PI-positive. As shown in Fig .4, The apoptotic rate of the control group of A549/DDP cells is 4.2% ± 0.8%, while the apoptotic rate of the A549/DDP cells treated with 0.5, 1.0, and 1.5 μg·mL^{-1} PPI for 24 h were 37.2% ± 4.4%, 49.2% ± 4.0%, and 65.1% ± 6.0%, respectively (Fig. 4A), and those of the A549/DDP cells treated with 0.5, 1.0, and 1.5 μg·mL^{-1} PVII for 24 h were 11.3% ± 1.0%, 25.0% ± 2.0%, and 55.7% ± 5.1%, respectively (Fig. 4B). These data demonstrate that PPI and PPVII induce apoptosis of A549/DDP cells in a dose dependent manner.

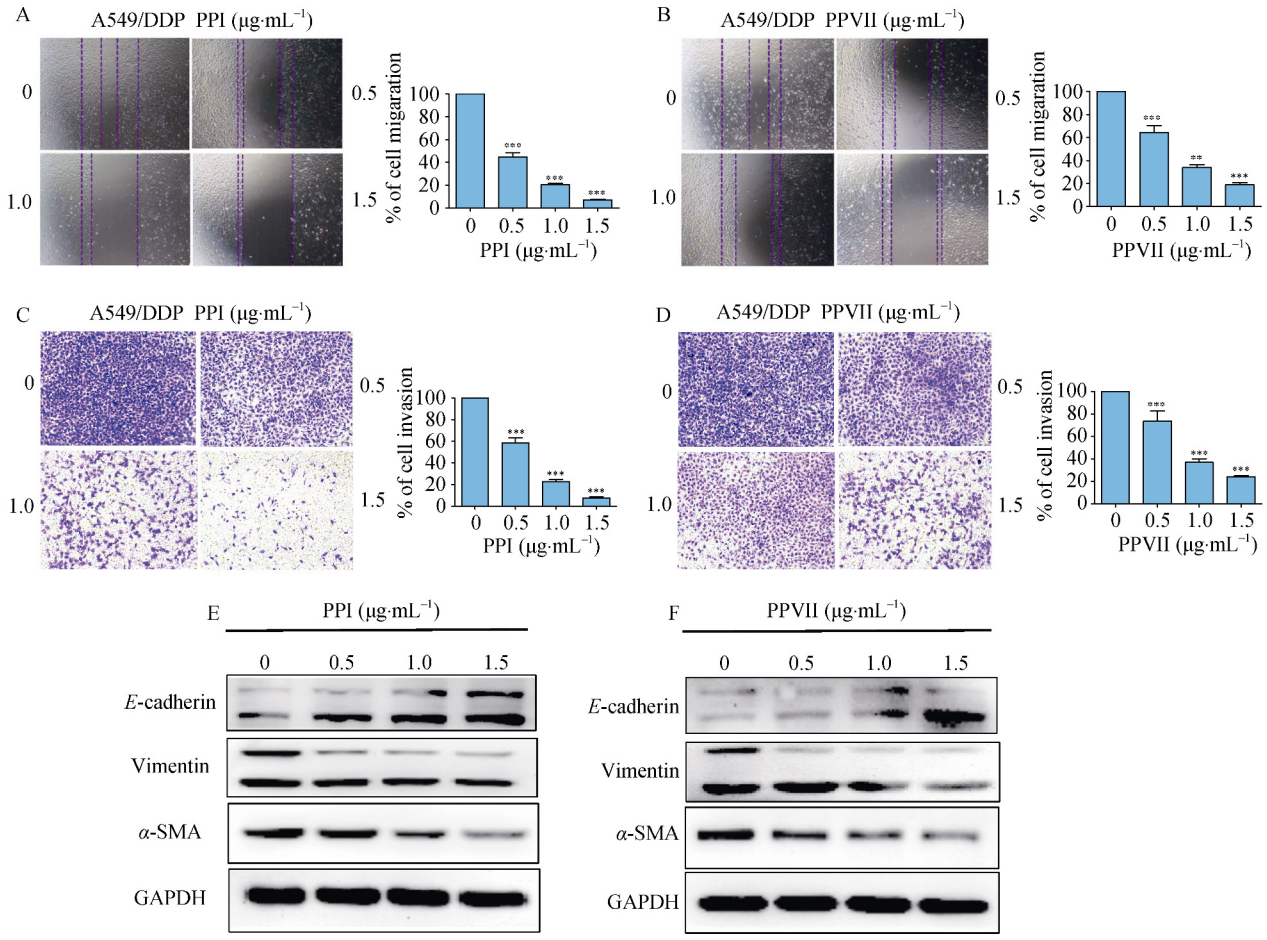

Fig. 3 PPI and PPVII inhibit migration, invasion and reverse EMT in A549/DDP cells. (A, B) Confluent cells were scratched and then treated with increasing concentrations of PPI (A) and PPVII (B) respectively for 24 h. (C, D) A549/DDP cells were treated with increasing concentrations of PPI (C) and PPVII (D) respectively for 24 h, then the invasion assay was evaluated. (E, F) A549/ DDP cells were treated with different concentrations of PPI (E) and PPVII (F) for 24 h respectively, then cells were harvested, the protein expression levels of *E*-cadherin, vimentin, *α*-SMA were measured by using western blot. $^{***}P$ < 0.001 *vs* control group

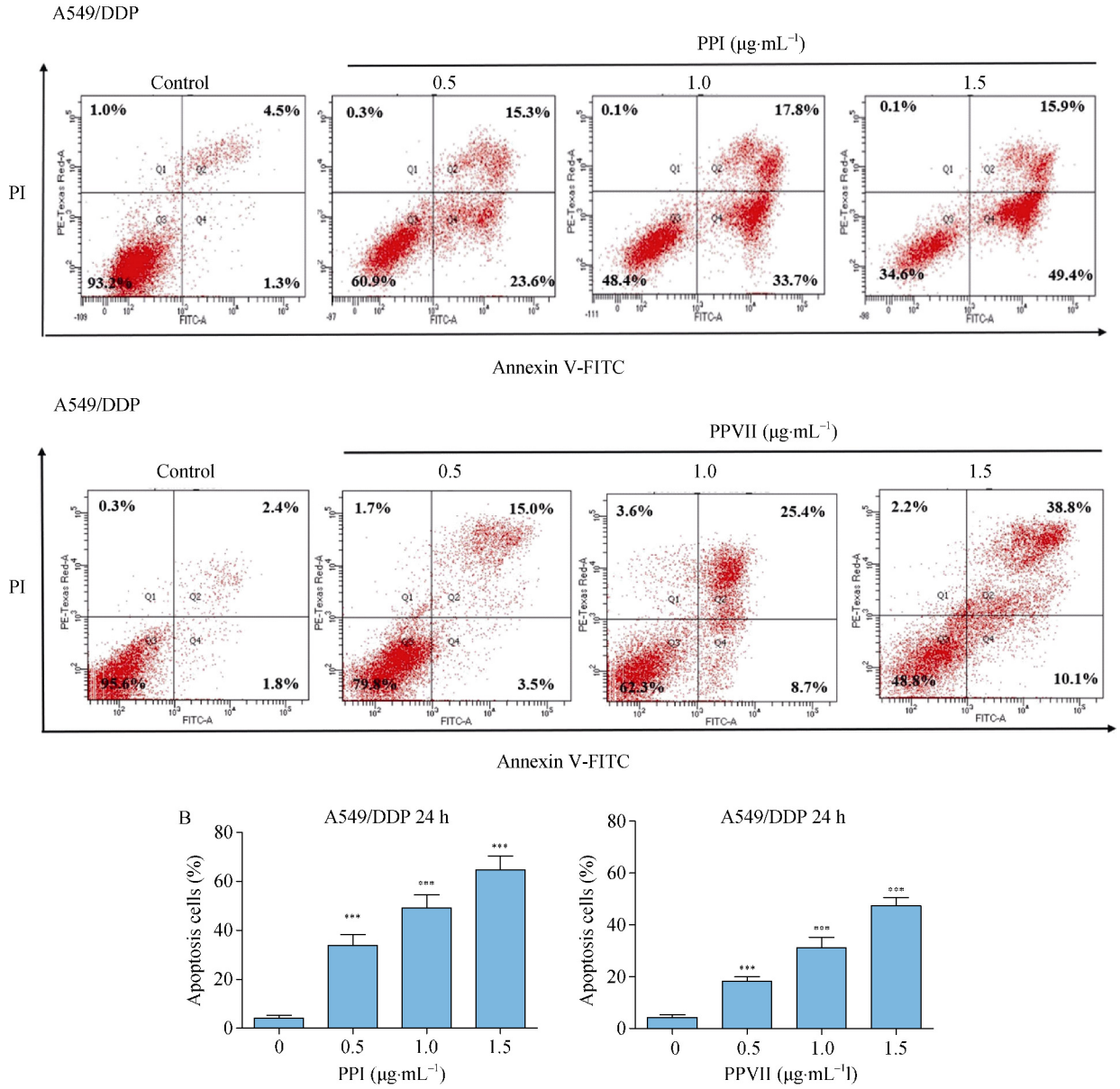

Fig. 4 The apoptosis effect induced by PPI and PPVII by Annexin V- FITC/PI apoptosis analysis. (A) A549/DDP cells were treated with 0.5, 1.0, 1.5 μg·mL^{-1} of PPI for 24 h respectively. (B) A549/DDP cells were treated with 0.5, 1.0, 1.5 μg·mL^{-1} of PPVII for 24 h respectively. Apoptosis of cells was detected by Annexin V-FITC/ PI staining and flow cytometry. The apoptotic percentage is shown as a bar graph. Data represents the mean ± SD of three independent experiments. $^{***}P < 0.001$, *vs* control group

PPI and PPVII induced apoptosis through the p53 pathway and caspases-dependent pathway.

In order to explore the mechanism by which PPI and PPVII induce apoptosis in A549/DDP cells, we examined the effects of PPI and PPVII on the expression of key regulators, including PARP, cleaved-PARP, p53, Bcl-2 family and caspases protein, which are the most important apoptosis regulators. Western blotting results showed that the PPI (Fig. 5A) and PPVII (Fig. 5B) up-regulated the expression of p53 and pro-apoptotic protein Bax, and down-regulated anti-apoptotic protein Bcl-2 expression, the ratio of Bax to Bcl-2 was significantly enhanced, which led to the activation of PARP, as well as activation of caspase-3, caspase-9, ultimately initiated cell apoptosis. We can see significant dose-dependent decrease in PARP and increase in cleaved-PARP, cleaved-caspase-3 and cleaved-caspase-9 in PPI (Fig. 5C) and PPVII (Fig. 5D) treated A549/DDP cells than in the control group. These results indicate that PPI and PPVII induced cell death *via* p53 pathway and caspase-dependent apoptosis.

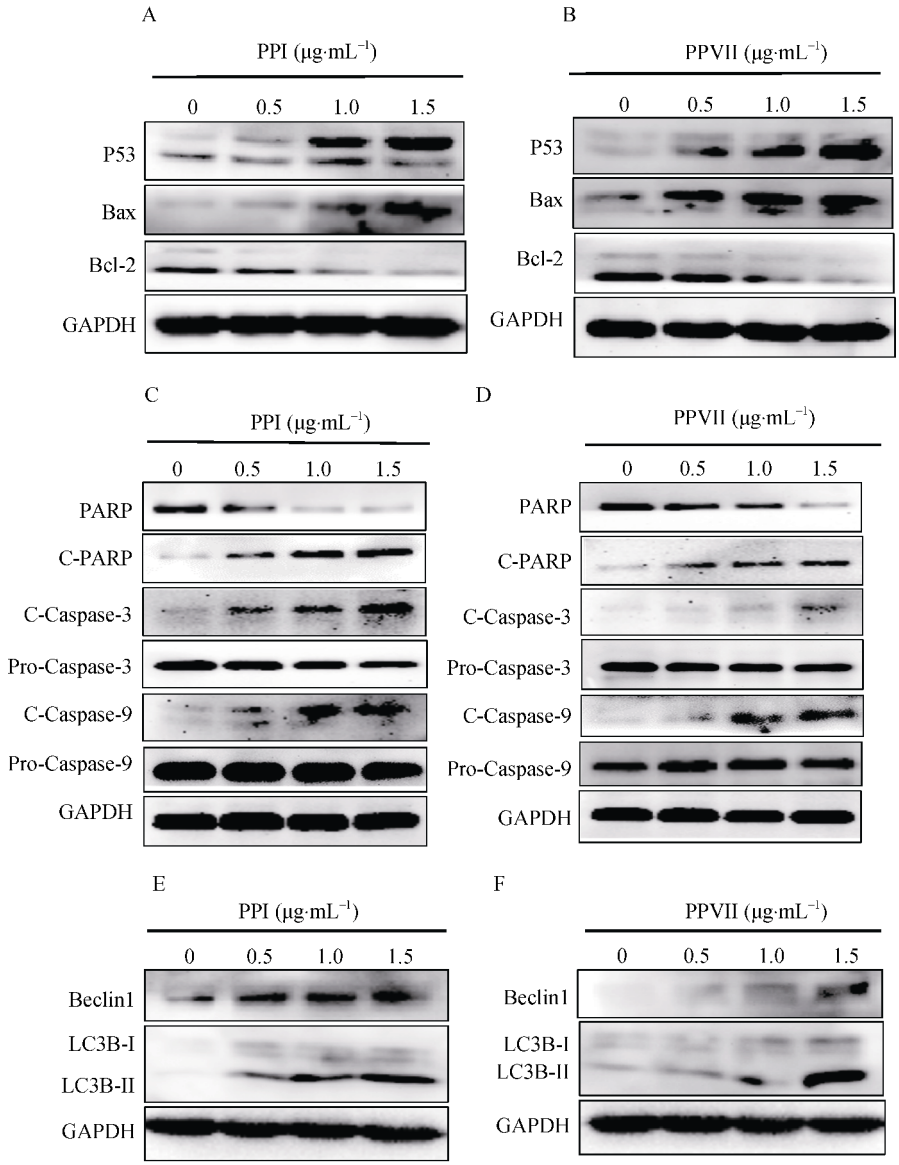

Fig. 5 PPI and PPVII induced apoptosis through the p53 pathway and caspases-dependent pathway (AcF). A549/DDP cells were treated with increasing concentrations of PPI and PPVII for 24 h, then cells were harvested, the protein expression levels of p53, Bcl-2, Bax (A, B) and PARP, cleaved-PARP, caspase-3, cleaved-caspase-3, caspase-9, cleaved-caspase-9 (C, D) and Beclin1, LC3B-I/II (E, F) were measured by using western blot

PPI and PPVII activate autophagy in A549/DDP cells

Autophagy, which has been classified as type 2 programmed cell death, is a lysosomal degradation process of cytoplasmic constituents under stress conditions. To determine whether autophagy is also involved in PPI and PPVII induced cell death, we subsequently evaluated the expression level of Beclin1 and LC3B of A549/DDP cells treated with PPI and PPVII using western blot. When autophagy occurs, LC3 is cut on the C-terminal and is converted from LC3B-I (the cytoplasmic form) into LC3B-II (the autophagosomic form).Western blot analysis showed that PPI (Fig. 5E) and PPVII (Fig. 5F) increased Beclin1 and LC3B-II levels in A549/DDP cells dose dependently, which confirmed that PPI and PPVII both activate autophagy in A549/DDP cells.

PPI and PPVII inhibits CIP2A and regulates the AKT/mTOR pathway.

CIP2A is an endogenous inhibitor of PP2A, which demonstrates tumor-promoting properties in NSCLC [4]. We detected the CIP2A expression and found that PPI (Fig. 6A) and PPVII (Fig. 6B) treatment significantly downregulated the expression of CIP2A in a time and dose dependent manner. The AKT pathway plays important roles in the growth, progression, survival, apoptosis, invasion, and metastasis of tumor cells, and AKT is a key locus of cancer multidrug resistance (MDR) and fragility [24]. The dephosphorylation of AKT is widely regulated by PP2A, therefore, we investigated the

effect of PPI and PPVII on AKT and AKT phosphorylation in A549/DDP cells.

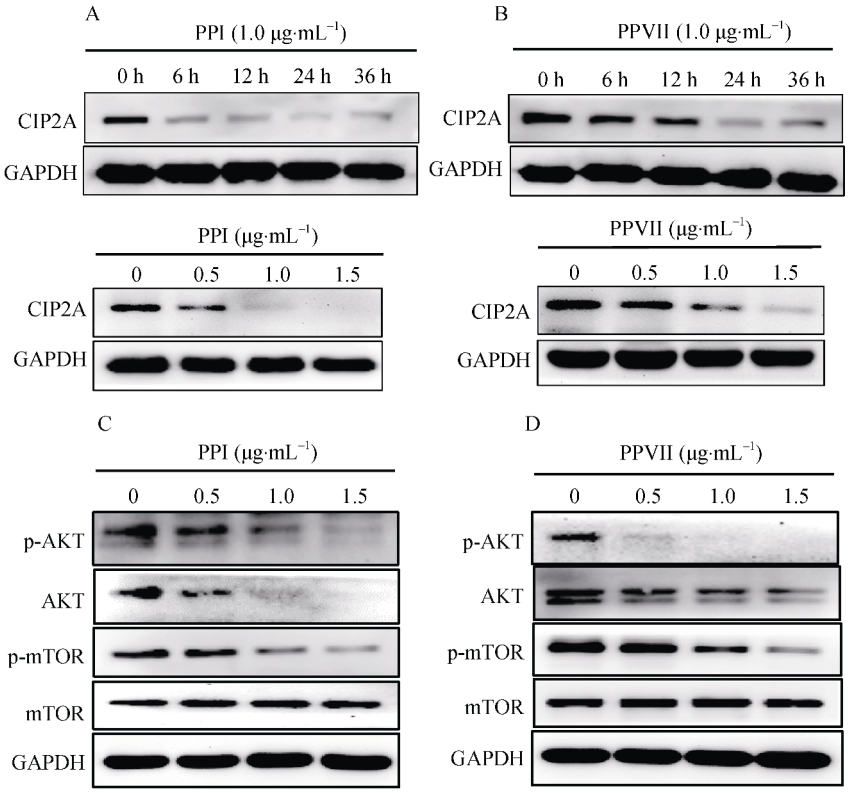

Fig. 6 PPI and PPVII suppressed CIP2A and suppressed AKT/mTOR signaling axis. (A, B) A549/DDP cells were incubated with different concentrations of PPI (A) or PPVII (B) for 24 h or treated with 1.0 μg·mL^{-1} PPI (A) or 1.0 μg·mL^{-1} PPVII (B) for indicated time points respectively, the protein expression levels of CIP2A were measured by using western blot. (C, D) A549/DDP cells were incubated with different concentrations of PPI (C) and PPVII (D) for 24 h respectively, the protein expression levels of p-AKT, AKT, p-mTOR, m-TOR were measured by using western blot.

Our results showed that the total AKT level and the phosphorylation level of AKT and was dose-dependently downregulated in the PPI (Fig. 6C) and PPVII (Fig. 6D) treated A549/DDP cells compared with the control group. The mTOR/p70S6K1 pathway is downstream of AKT in mediating cisplatin resistance in lung cancer cells [25]. mTOR is also the major negative regulator of autophagy and its activation results in phosphorylation of important effectors involved in cancer progression and apoptosis resistance [9]. Thus, we determined the changes in the expression of mTOR and phosphorylation level of mTOR, the results suggested that PPI (Fig. 6C) and PPVII (Fig. 6D) could significantly downregulated the expression of the phosphorylation level of mTOR. These results suggest that PPI and PPVII may affect the CIP2A/AKT/mTOR signaling axis.

Discussion

The present study first identified the significant inhibitory effects of natural compounds PPI and PPVII inhibiting DDP-resistant NSCLC and to gain insight regarding the molecular mechanism. Our data indicated that PPI and PPVII inhibited the growth of NSCLC cell lines A549 and cisplatin-resistant A549/DDP cells at low IC50 values in a dose-dependent manner (Table 1). Besides, A549/DDP were more sensitive to PPI and PPVII treatment (Fig. 1), suggesting their worth of further investigation. Thus, we investigated the effect and mechanism of PPI and PPVII on A549/DDP cells.

Table 1 IC_{50} (μg·mL^{-1}) of PPI and PPVII on NSCLC cell lines (means ± SD, n = 4)

Cell lines	A549	A549/DDP
PPI	1.54 ± 0.26	1.08 ± 0.20
PPVII	2.26 ± 0.30	1.84 ± 0.23

The cells were treated with PPI and PPVII at various concentrations for 24 h, the cell cytotoxicity was analyzed by CCK-8 assay, and the IC_{50} was calculated using SPSS (version 19.0).

EMT is a process that tumor cells lose their cell to cell junctions and acquire mesenchymal properties, such as cell migration and invasion [26]. Besides, much work has found that EMT is associated with the emergence of drug resistance, consequently, reversing EMT to suppress cancer metastasis and delay or prevent drug resistance is considered a potential therapeutic option for cancer. In this study, we demonstrated

that PPI and PPVII treatment inhibited cell migration, invasion (Figs. 3A–3D) and reversed EMT process of A549/DDP cells, evidenced by upregulation of the epithelial marker *E*-cadherin and downregulation of the mesenchymal marker vimentin and *α*-SMA (Figs. 3E and 3F); thus, PPI and PPVII exerted anti-invasive activities partly by reversing EMT in DDP-resistant NSCLC cells.

Apoptosis, consisting of extrinsic and intrinsic pathways, is the main cell death response to chemotherapy. One of the symbols of chemoresistance is evading apoptosis and targeting apoptosis has become a therapeutic strategy of cancer [27-28]. To examine whether the anti-proliferative effects of PPI and PPVII were related to apoptosis induction, A549/DDP cells were treated with PPI and PPVII for 24 h, followed by Annexin V-FITC/ PI staining and flow cytometry. The results demonstrated that PPI and PVII significantly increased the apoptosis rate in A549/DDP cells in a dose dependent manner (Figs. 4A and 4B). The extrinsic and intrinsic apoptotic pathways that ultimately lead to activation of effector caspase-3 have been characterized [29]. We further examined the effects of PPI or PPVII on the expression of key apoptosis regulators and results showed that PPI and PPVII treatment significantly up-regulated the expression of p53 and Bax, and down-regulated Bcl-2 expression (Figs. 5A and 5B), the ratio of Bax to Bcl-2 was significantly enhanced, which led to the activation of PARP, as well as activation of caspase-3, caspase-9, reflected by a decrease of PARP and increase of cleaved-PARP, cleaved-caspase-3 and cleaved-caspase 9 (Figs. 5C and 5D), ultimately initiated cell apoptosis. These results indicate that PPI and PPVII induced p53 evoked and caspase-dependent apoptosis in A549/DDP cells. Autophagy is considered as type 2 programmed cell death which plays an important role in cancer progression and chemoresistance [30]. When autophagy occurs, LC3 is cut on the C-terminal and is converted from the cytoplasmic form LC3B-I into the autophagosomic form LC3B-II. Beclin1 functions as the key factor in the autophagosomes formation [31]. Our present results illustrated that PPI and PPVII activated autophagy by the upregulation of LC3B-Ⅱ and Beclin1 levels (Figs. 5E and 5F).

CIP2A is an oncoprotein with many important roles in biological functions of tumorigenesis chemoresistance. Overexpression of CIP2A is found at a high frequency in multiple cancer types and is associated with poor prognosis [3-7]. CIP2A performs an ‘oncogenic nexus’ by participating in multiple pathways, including the PI3K-AKT, RAS/ERK and the Wnt/ *β*-catenin pathway [6]. The functions of CIP2A in apoptosis and autophagy are not fully understood yet. Previous studies proved that CIP2A depletion or downregulation contributes to cell apoptosis in several cancer types [11, 32-33]. Functional studies also confirmed the potential role of CIP2A depletion or downregulation in sensitizing cancer cells to several chemotherapeutic agents, including cisplatin [33-34]. In the present study, PPI and PPVII suppressed the expression of CIP2A in a time and dose dependent manner and then inhibited the CIP2A downstream AKT/mTOR signaling cascade (Fig. 6). PPI and PPVII also significantly upregulated the expression of p53 and induce caspase-dependent apoptosis finally (Fig. 5). As a tumor suppressor, p53 is activated in response to DNA-damaging stress, which can induce apoptosis or either transient or permanent cell cycle arrests. p53 has complicated interactions with CIP2A *via* PPP2R1A [6], and there is also abundant crosstalk between p53 and AKT/mTORC1 signaling pathway, and this crosstalk can determine the choice of cell response to p53 [35], which needs our further exploration. As for the autophagy, Puustinen *et al* reported that CIP2A promotes cell growth and inhibits autophagy through CIP2A/PP2A/mTORC1 signaling axis. CIP2A can associate with mTORC1 and act as an allosteric inhibitor of mTORC1-associated PP2A, resulted in enhancement of mTORC1-dependent growth signaling and autophagy inhibition [36]. Moreover, the mTOR/p70S6K1 pathway is downstream of AKT in mediating cisplatin resistance in lung cancer cells [25]. Our present study demonstrated that PPI and PPVII promoted the formation of autophagy *via* the inhibition of mTOR, which may also have effect on cisplatin resistance in lung cancer. The functions of CIP2A in EMT are also not fully understood yet. Overexpression of CIP2A promotes EMT process [6, 37]. Wu *et al* reported that CIP2A cooperates with H-Ra *via* the MEK/ERK pathway, which promotes EMT and cervical cancer progression [8]. Base on the above research, we propose that PPI and PPVII inhibit the invasion and EMT of A549/DDP cells by the downregulation of CIP2A.

In conclusion, PPI and PVII exhibited strong inhibitory effects on A549/DDP lung cancer cell growth *in vitro*, inducing apoptosis and autophagy and reversing EMT in human cisplatin resistant NSCLC cells *via* p53 upregulation and CIP2A/AKT/mTOR signaling axis inhibition. PPI and PPVII might be developed as potential chemotherapeutic drugs in NSCLC especially the DDP-resistant NSCLC therapy in the future.

References

[1] Siegel RL, Miller KD, Jemal A. Cancer statistics, 2017 [J]. *CA Cancer J Clin*, 2017, **67**(1): 7-30.

[2] Szejniuk WM, Robles AI, McCulloch T, *et al*. Epigenetic predictive biomarkers for response or outcome to platinum-based chemotherapy in non-small cell lung cancer, current state-of-art [J]. *Pharmacogenomics J*, 2019, **19**(1): 5-14.

[3] Junttila MR, Puustinen P, Niemelä M, *et al*. CIP2A inhibits PP2A in human malignancies [J]. *Cell*, 2007, **130**(1): 51-62.

[4] Liu Z, Ma L, Wen ZS, *et al*. Cancerous inhibitor of PP2A is targeted by natural compound celastrol for degradation in non-small-cell lung cancer [J]. *Carcinogenesis*, 2014, **35**(4): 905-914.

[5] Liu CY, Shiau CW, Kuo HY, *et al*. Cancerous inhibitor of protein phosphatase 2A determines bortezomib-induced apoptosis in leukemia cells [J]. *Haematologica*, 2013, **98(5)**: 729-738.

[6] De P, Carlson J, Leyland-Jones B, *et al*. Oncogenic nexus of cancerous inhibitor of protein phosphatase 2A (CIP2A): An

oncoprotein with many hands [J]. *Oncotarget*, 2014, **5**(13): 4581-602.

[7] Tang M, Shen JF, Li P1, *et al*. Prognostic significance of CIP2A expression in solid tumors: A meta-analysis [J]. *PLoS One*, 2018, **13**(7): e0199675.

[8] Wu Y, Gu TT, Zheng PS, *et al*. CIP2A cooperates with H-Ras to promote epithelial-mesenchymal transition in cervical-cancer progression [J]. *Cancer Lett*, 2015, **356**(2 Pt B): 646-655.

[9] Wu WD, Hu ZM, Shang MJ, *et al*. Cordycepin down-regulates multiple drug resistant (MDR)/HIF-1α through regulating AMPK/mTORC1 signaling in GBC-SD gallbladder cancer cells [J]. *Int J Mol Sci*, 2014, **15**(7): 12778-12790.

[10] Lin YC, Chen KC, Chen CC, *et al*. CIP2A-mediated Akt activation plays a role in bortezomib-induced apoptosis in head and neck squamous cell carcinoma cells [J]. *Oral Oncol*, 2012, **48**(7): 585-593.

[11] Yu HC, Chen HJ, Chang YL, *et al*. Inhibition of CIP2A determines erlotinib-induced apoptosis in hepatocellular carcinoma [J]. *Biochem Pharmacol*, 2013, **85**(3): 356-366.

[12] Zhang X, Xu B, Sun C, *et al*. Knockdown of CIP2A sensitizes ovarian cancer cells to cisplatin: an *in vitro* study [J]. *Int J Clin Exp Med*, 2015, **8**(9): 16941-16947.

[13] Ho JW, Leung YK, Chan CP, *et al*. Herbal medicine in the treatment of cancer [J]. *Curr Med Chem Anticancer Agents*, 2002, **2**(2): 209-214.

[14] Entidhar Al Sawah, Douglas C, Marchion, *et al*. The Chinese herb polyphyllin D sensitizes ovarian cancer cells to cisplatin-induced growth arrest [J]. *J Cancer Res Clin Oncol*, 2015, **141**(2): 237-242.

[15] Shi YM, Yang L, Geng YD, *et al*. Polyphyllin I induced-apoptosis is enhanced by inhibition of autophagy in human hepatocellular carcinoma cells [J]. *Phytomedicine*, 2015, **22**(13): 1139-1149.

[16] Gu LH, Feng JG, Zheng ZG, *et al*. Polyphyllin I inhibits the growth of ovarian cancer cells in nude mice [J]. *Oncol Lett*, 2016, **12**(6): 4969-4974.

[17] Chang J, Li Y, Wang X, *et al*. Polyphyllin I suppresses human osteosarcoma growth by inactivation of Wnt/β-catenin pathway *in vitro* and *in vivo* [J]. *Sci Rep*, 2017, **7**(1): 7605.

[18] Kong MJ, Fan JQ, Dong AQ, *et al*. Effects of polyphyllin I on growth inhibition of human non-small lung cancer cells and in xenograft [J]. *Acta Biochim Biophys Sin*, 2010, **42**(11): 827-833.

[19] Dong RZ, Guo JM, Zhang ZW, *et al*. Polyphyllin I inhibits gastric cancer cell proliferation by downregulating the expression of fibroblast activation protein alpha (FAP) and hepatocyte growth factor (HGF) in cancer-associated fibroblasts [J]. *Biochem Biophys Res Commun*, 2018, **497**(4): 1129-1134.

[20] Cai XQ, Guo LL, Pei F, *et al*. Polyphyllin G exhibits antimicrobial activity and exerts anticancer effects on human oral cancer OECM-1 cells by triggering G_2/M cell cycle arrest by inactivating cdc25C-cdc2 [J]. *Arch Biochem Biophys*, 2018, **644**: 93-99.

[21] Zhang C, Jia XJ, Bao JL, *et al*. Polyphyllin VII induces apoptosis in HepG2 cells through ROS-mediated mitochondrial dysfunction and MAPK pathways [J]. *BMC Complement Altern Med*, 2016, **16**: 58.

[22] Lin ZF, Liu YT, Li FY, *et al*. Anti-lung cancer effects of polyphyllin VI and VII potentially correlate with apoptosis *in vitro* and *in vivo* [J]. *Phytother Res*, 2015, **29**(10): 1568-1576.

[23] Nurwidya F, Takahashi F, Murakami A, *et al*. Epithelial mesenchymal transition in drug resistance and metastasis of lung cancer [J]. *Cancer Res Treat*, 2012, **44**(3): 151-156.

[24] Radisavljevic Z. AKT as locus of cancer multidrug resistance and fragility [J]. *J Cell Physiol*, 2013, **228**(4): 671-674.

[25] Liu LZ, Zhou XD, Qian G, *et al*. AKT1 amplification regulates cisplatin resistance in human lung cancer cells through the mammalian target of rapamycin/p70S6K1 pathway [J]. *Cancer Res*, 2007, **67**(13): 6325-6332.

[26] Brabletz T, Kalluri R, Nieto MA, *et al*. EMT in cancer [J]. *Nat Rev Cancer*, 2018, **18**(2): 128-134.

[27] Koji F, Hisakazu I, Kyoko O, T*et al*. Cancer therapy due to apoptosis: galectin-9 [J]. *Int J Mol Sci*, 2017, **18**(1): E74.

[28] Hassan M, Watari H, AbuAlmaaty A, *et al*. Apoptosis and molecular targeting therapy in cancer [J]. *Biomed Res Int*, 2014, **2014**: 150845.

[29] Nicholson DW. Caspase structure, proteolytic substrates, and function during apoptotic cell death [J]. *Cell Death Differ*, 1999, **6**(11): 1028-1042.

[30] Taylor MA, Das BC, Ray SK. Targeting autophagy for combating chemoresistance and radioresistance in glioblastoma [J]. *Apoptosis*, 2018, **23**(11-12): 563-575.

[31] Jin HO, Hong SE, Park JA, *et al*. Inhibition of JNK-mediated autophagy enhances NSCLC cell sensitivity to mTORC1/2 inhibitors [J]. *Sci Rep*, 2016, **6**: 28945.

[32] Lan Jin, Yuan S, Xing Hong, *et al*. Ethoxysanguinarine inhibits viability and induces apoptosis of colorectal cancer cells by inhibiting CIP2A [J]. *Int J Oncol*, 2018, **52**(5): 1569-1578.

[33] Gao F, Wang X, Chen S, *et al*. CIP2A depletion potentiates the chemosensitivity of cisplatin by inducing increased apoptosis in bladder cancer cells [J]. *Oncol Rep*, 2018, **40**(5): 2445-2454.

[34] Xu P, Yao J, He J, *et al*. CIP2A down regulation enhances the sensitivity of pancreatic cancer cells to gemcitabine [J]. *Oncotarget,* 2016, **7**(12): 14831-14840.

[35] Duan L, Maki CG. The IGF-1R/AKT pathway determines cell fate in response to p53 [J]. *Transl Cancer Res*, 2016, **5**(6): 664-675.

[36] Puustinen P, Rytter A, Mortensen M, *et al*. CIP2A oncoprotein controls cell growth and autophagy through mTORC1 activation [J]. *J Cell Biol*, 2014, **204**(5): 713-727.

[37] Pang X, Fu X, Chen S, *et al*. Overexpression of CIP2A promotes bladder cancer progression by regulating EMT [J]. *Clin Transl Oncol*, 2016, **18**(3): 289-295.

Cite this article as: FENG Fei-Fei, CHENG Peng, SUN Chao, WANG Hui, WANG Wei. Inhibitory effects of polyphyllins I and VII on human cisplatin-resistant NSCLC *via* p53 upregulation and CIP2A/AKT/mTOR signaling axis inhibition [J]. *Chin J Nat Med*, 2019, **17**(10): 768-777.